JOURNAL OF MATERIALS SCIENCE 29 (1994) 1966–1972

Diels–Alder reaction of mesophase pitch insoluble fractions with maleic anhydride

H. TOSHIMA, T. HINO, K. MURAKAMI
Corporate Research and Development Laboratory, Tonen Co. Ltd, 1-3-1, Nishi-Tsurugaoka, Iruma, Saitama 354, Japan

I. MOCHIDA
Institute of Advanced Material Study, Kyushu University, 6-1, Kasuga, Fukuoka 816, Japan

Pyridine insoluble fractions in the mesophase pitches derived from a decant oil (PMP-PI) and naphthalene (NMP-PI) were found to be rendered almost completely soluble in pyridine by the Diels–Alder reaction with maleic anhydride, maintaining their optical anisotropy and molecular association. Their solubility in pyridine reached up to 95 wt % by the reaction at 175–200 °C. Solubilized fractions were analysed to obtain their average structures, suggesting that PMP-PI consists of aromatic nuclei of peri-condensed rings connected through a small number of methylene and aryl–aryl linkages, having a molecular weight (MW) of ~ 1800, and that NMP-PI consists of oligomeric naphthalene with a large number of naphthenic groups (MW $\simeq 1000$). Such structures are basically much the same as those of their soluble fractions, although the molecules in PIs were much larger. The reaction sites in such structures for the Diels–Alder reaction are discussed.

1. Introduction

The mesophase pitch has been recognized for sometimes as one of the unique precursors for the advanced carbon materials, such as high-performance carbon fibre [1]. Its better performances are extensively pursued to achieve better quality of the product. The chemical structures of all the components in the pitch should be clarified in order to design the desirable properties [2–7].

The mesophase pitch consists of several fractions of different solubilities [1–8]. Soluble and lighter fractions have been analysed to determine the structures of their components, using various modern analytical instruments such as nuclear magnetic resonance (NMR) and vapour pressure osmometry (VPO) [6, 9–12]. Insoluble fractions should be solubilized before analysis. Reductive hydrogenation and alkylation, such as Birch reduction, have been applied extensively, although these procedures are rather tedious [13–15]. Simpler reactions are wanted.

Diels–Alder reaction has been applied for the solubilization of coal and suggests the presence of noncovalent bonds in its structure [16, 17]. The reaction proceeds simply by heating the mixture of coal and dienophiles, such as maleic anhydride. The conjugated double bonds in the aromatic ring, such as 9,10 positions of anthracene, are known to be reactive for the Diel–Alder reaction as described by the following equation. Such an adduct may obtain higher solubility.

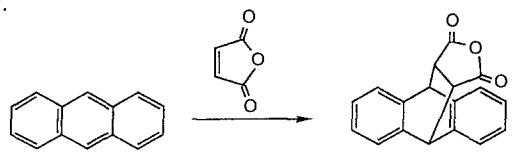

(1)

In the present study, the Diels–Alder reaction of a pyridine insoluble fraction in petroleum and naphthalene-derived mesophase pitches was performed to solubilize the fractions for analysis of their structures. The adducts may be deformed from planar to bent structure, weakening the interaction between aromatic planes in the mesophase pitch. Such a structural modification may have further interest, since it may control the properties of the mesophase pitch as the liquid crystal.

2. Experimental procedure

2.1. Materials

Two kinds of mesophase pitch derived from fluidized catalytic cracking-decant oil (FCC–DO) [18] and naphthalene [9, 10] were used as the starting materials in the present study. The former mesophase pitch (PMP) was prepared through the heat treatment of the FCC-DO at 415 °C and successive hot centrifugation at 350 °C to concentrate the mesophase components from the isotropic matrix. The latter pitch (NMP) was prepared through the cationic polymerization of naphthalene with a super acid of HF/BF_3, which was supplied by Mitsubishi-Gas Chemical Company.

The pyridine insoluble fractions (PI) of petroleum (FCC–DO derived) and naphthalene-derived mesophase pitches (abbreviated PMP-PI and NMP-PI, respectively) were prepared by Soxhlet extraction.

2.2. The Diels–Alder reaction

The maleic anhydride was selected as a dienophile reagent for the present Diels–Alder reaction [16, 17].

0022–2461

The powder of PI fraction (2g) was well mixed with maleic anhydride (8g) at room temperature and then heat treated in a glass tube in a vertical electric furnace at 130–200 °C for 1 h under a nitrogen flow (50 ml min^{-1}). The heating rate to the prescribed temperature was 5 °C min^{-1}. The reaction proceeded in the suspension state of PI in the melted maleic anhydride. After the reaction, the product was first heated at 60 °C under vacuum and then washed with methanol to remove the unreacted maleic anhydride from the reacted pitch fraction.

2.3. Characterization of PI after the reaction

The modified PI fractions (DA-PIs) were characterized by elemental analyses, solubility in pyridine and quinoline, optical microscopy, wide-angle X-ray diffraction (XRD), Fourier transform–infrared analysis (FT–IR), vapour pressure osmometry (VPO), and ^{1}H-NMR to clarify the structures and properties of the fractions.

The solubility in pyridine and quinoline (4 ml) was measured, using 1.0 g sample by a Soxhlet and extraction/filtration at 80 °C, respectively.

The molecular association of the reacted PI fractions was measured using wide-angle X-ray diffraction. The following equations [19] were applied for the analyses

$$L_c(002) = K\tilde{N}\lambda/\tilde{N}\cos\theta \quad (2)$$

$$d(002) = \lambda/2\tilde{N}\sin\beta \quad (3)$$

where $K = 1.0$, $\lambda = 1.05418$ nm, θ is calculated from the (0 0 2) diffraction angle 2θ, and β is the full-width at half maxium (FWHM) of the diffraction profile. The functional groups of the pitches were characterized with FT–IR (Jeol JIR-100) by the KBr disc method.

The average molecular weights of the solubilized fractions in the adducts were measured by VPO, using pyridine as the solvent. The pyridine-soluble fractions in the pitches were also characterized with ^{1}H–NMR (Jeol JNM–GSX400) in the C_5D_5N solution, using tetramethysilane (TMS) as an internal standard, to measure the hydrogen distributions and calculate the Brown–Ladner structural parameters of the fractions [20]. The molar number of the adducted maleic anhydride in the solubilized fraction was estimated from the elemental analyses and average molecular weight of the fraction. The hydrogen distributions of the solubilized fractions were also estimated by subtracting the contribution of the adducted maleic anhydride.

3. Results

3.1. Some analyses of parent PI fractions

Some analytical data of the parent PI fractions in both mesophase pitches are summarized in Table I. The petroleum-derived mesophase pitch (PMP) contained a higher content of PI fraction and PMP-PI had a lower atomic H/C ratio, and a higher carbon aromaticity, f_a, than that of the naphthalene-derived mesophase pitch (NMP-PI) [21].

The FT–IR spectra of both PI fractions are shown in Fig. 1. The bands around 2960–2850 and 1450–1360 cm^{-1}, which are ascribed to the aliphatic C–H stretching vibration, were much more intense with NMP-PI than with PMP-PI. The bands around 870–750 cm^{-1} (the aromatic C–H groups) were also much more intense with NMP-PI. These results suggest that the NMP-PI carries more cata-condensed structures and a greater content of aliphatic and naphthenic groups.

3.2. Properties of modified PI (DA-PI)

Fig. 2 shows the optical micrographs of the parent and reacted PI fractions. The parent PMP-PI showed the large domains of anisotropy and sharp particle edges. Although the PMP-PI reacted at 150 °C for 1 h showed the same amsotropy, some particles certainly became much smaller and round, as shown in Fig. 2c (i) and (ii).

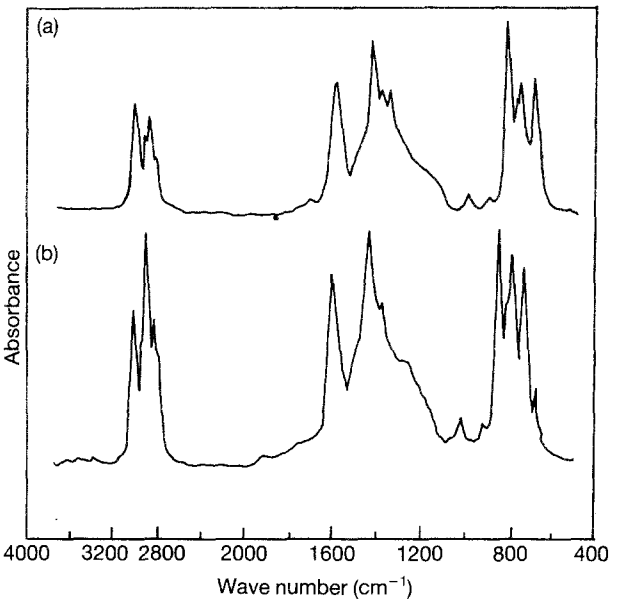

Figure 1 FT–IR spectra of the parent PI fractions in PMP and NMP. (a) PMP-PI, (b) NMP-PI.

TABLE I Some analyses of parent pyridine insoluble fractions (PIs)

Sample	PI yield[a] (wt %)	Element (wt %)				H/C	O/C ($\times 10^{-3}$)	f_a[b]
		C	H	O	Diff.			
PMP-PI[c]	51	93.8	4.0	0.9	1.3	0.51	7.2	0.92
NMP-PI[d]	37	93.8	4.3	0.7	1.2	0.55	5.6	0.88

[a] Based upon the parent mesophase pitch.
[b] Estimated by elemental analyses and FT–IR.
[c] PI fraction of petroleum (FCC-DO)-derived mesophase pitch.
[d] PI fraction of naphthalene-derived mesophase pitch.

TABLE II Some properties of parent and reacted PI fractions

Sample	Reaction conditions	Solubilities (%)		Optical texture	SP (°C)[a]	XRD parameters (nm)	
		PS	QS			L_{c002}	d_{002}
PMP-PI	–	0	13	Anisotropy	450	4.0	0.3464
	150 °C,1 h	40	84	Anisotropy	452	3.6	0.3464
	175 °C,1 h	73	97	Anisotropy	455	4.3	0.3462
NMP-PI	–	0	4	Anisotropy	430	3.7	0.3490
	150 °C,1 h	74	84	Anisotropy	438	4.3	0.3479
	175 °C,1 h	90	97	Anisotropy	450	4.3	0.3497

[a]Measured by hot-stage equipment attached to the polarized-light microscope.

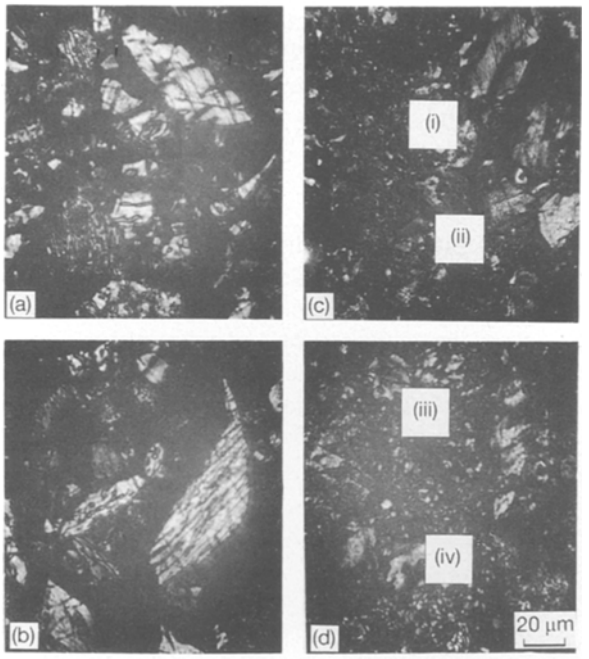

Figure 2 Optical micrographs of the PI fractions (a,b) before and (c,d) after the Diels–Alder reaction. (a,c) PMP-PI, (b,d) NMP-PI.

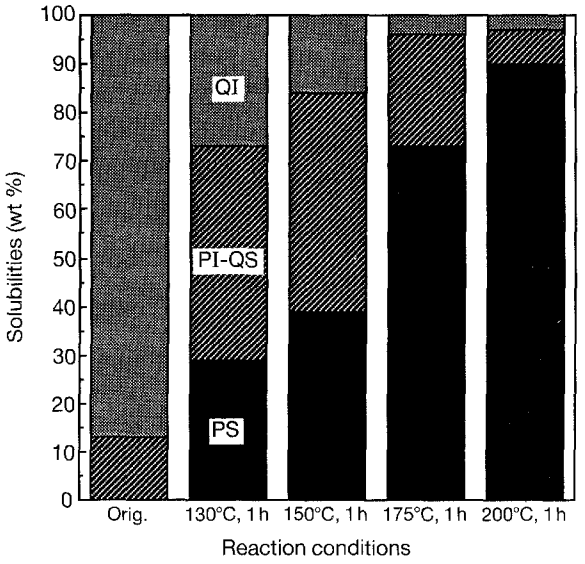

Figure 3 Solubilities of the PMP-PI fraction after the Diels–Alder reaction with maleic anhydride.

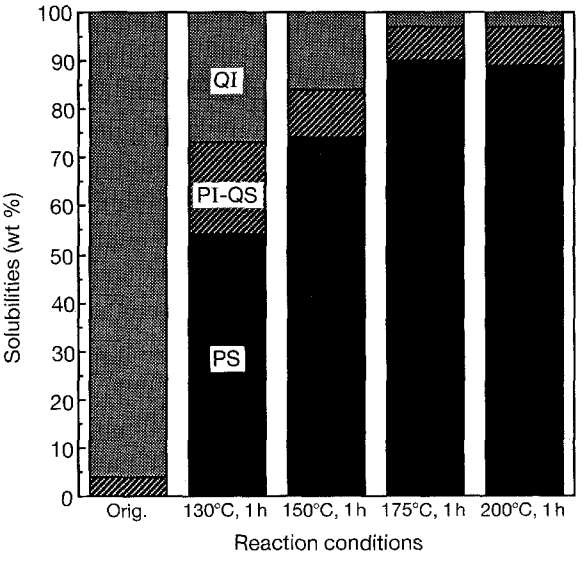

Figure 4 Solubilities of the NMP-PI fraction after the Diels–Alder reaction with maleic anhydride.

NMP-PI showed the same optical morphology before and after the Diels–Alder reaction as shown in Fig. 2d (iii) and (iv), although the particles of the fraction were much finer than those of PMP-PI. The PI particles are suggested to be dissolved, at least at their edges, in the melted maleic anhydride during the reaction at elevated temperatures.

Table II summarizes the properties of the reacted PI fractions. The optical anisotropy was always maintained in every fraction produced after the Diels–Alder reaction. The softening point of both PI fractions after the reaction became higher, the increase of the softening point being larger with NMP-PI.

The stacking height, $L_c(0\,0\,2)$, and the $d(0\,0\,2)$ spacing of both PIs were much the same before and after the reaction, although a slight change was observable.

3.3. Solubilities of modified PI (DA-PI) fractions

Solubilities of the PI fractions in pyridine and quinoline after the Diels–Alder reaction with maleic anhydride are summarized in Figs 3 and 4, where the reactions were carried out at 130–200 °C for 1 h.

The reaction certainly enhanced the solubilities in pyridine and quinoline. The pyridine-soluble (PS) content of PMP-PI reached 90 wt % on reaction at 200 °C, as shown in Fig. 3. No further increase of the PS yield was observable with still higher temperatures. The quinoline-soluble (QS) content was also steadily

increased by the reaction as QS content reached 97 wt % at 200 °C.

The PS and QS contents of the NMP-PI after the reaction also increased, as shown in Fig. 4. The higher solubility was obtained with the fraction at lower temperatures than those of PMP-PI. The reaction temperatures of 130 and 150 °C provided the solubility in pyridine of 55 and 73 wt %, respectively. The solubility increased to 90 wt % after reaction at 175 °C. QS increased to 97 % at 175 and 200 °C.

3.4. Characterization of PI and solubilized PI fractions

Fig. 5 illustrates the oxygen contents of the PI fractions after the Diels–Alder reaction with maleic anhydride. The oxygen content of PMP-PI increased steadily with the reaction temperatures. The oxygen contents after reaction at 130 and 150 °C were around 5 and 8 wt %, respectively. The content markedly increased to 22 and 30 wt % on reaction at 175 and 200 °C, respectively. The oxygen content of NMP-PI increased similarly. However, the contents were much larger than those of PMP-PI fractions at the same reaction temperatures. The oxygen contents reached 27 and 33 wt % on reaction at 150 and 175 °C, respectively. No increase in oxygen content was observed at still higher temperatures, as with solubility.

Figs 6 and 7 show the FT–IR spectra of the PI fractions before and after the Diels–Alder reaction. Intense bands were observed at around 1860, 1780 and 1740 cm^{-1}, and around 1220 cm^{-1}, which were ascribed to the carbonyl and ether bonds of the adducted maleic anhydride, respectively. Correspondingly, three bands around 870–750 cm^{-1} (the aromatic C–H vibrations) were weakened after the reaction. Such changes in the spectra were more marked by reaction at higher temperatures.

The same features were observable with NMP-PI after the Diels–Alder reaction, as shown in Fig. 7. However, the intensity of the oxygen functional groups and aromatic C–H groups was larger and

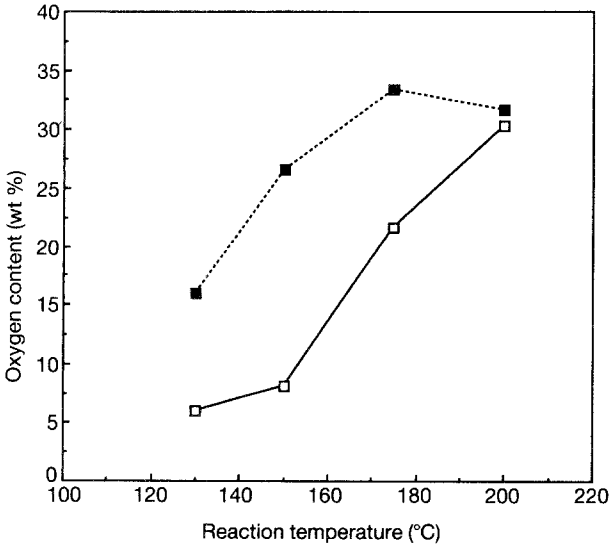

Figure 5 Oxygen contents of (□) PMP-PI and (■) NMP-PI fractions after the Diels–Alder reaction with maleic anhydride.

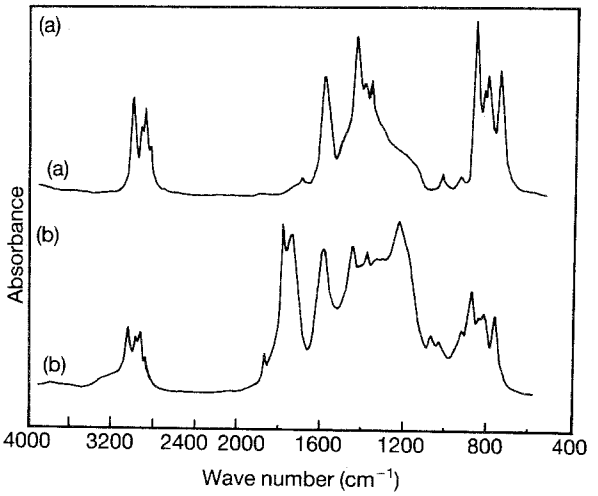

Figure 6 FT–IR spectra of the PMP-PI fraction before and after the Diels–Alder reaction; (a) PMP-PI, (b) PMP-PI reacted at 150 °C for 1 h.

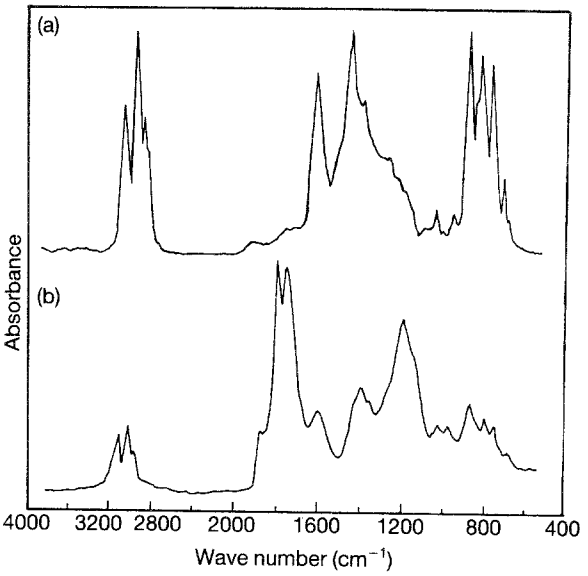

Figure 7 FT–IR spectra of the NMP-PI fraction before and after the Diels–Alder reaction; (a) NMP-PI, (b) NMP-PI reacted at 150 °C for 1 h.

smaller, respectively, in the reacted NMP-PI fraction than those of PMP-PI, suggesting much more extensive reaction in the NMP-PI under the same conditions.

The soluble fractions in pyridine of the PMP-PI and NMP-PI after reaction at 175 and 150 °C, respectively, were characterized by elemental analyses, VPO and ^{1}H–NMR to clarify their respective chemical structures. Table III summarizes elemental analyses, average molecular weight and molar number of the adducted maleic anhydride in the fractions. As shown in Table III, the same solubility around 73 wt% was observable with both fractions, in spite of a lower temperature with NMP-PI. Both oxygen content and atomic O/C ratio were higher with the fraction in NMP-PI. The average molecular weight of the fractions in PMP-PI was much larger (2520) than that of NMP-PI (1740).

The average molar numbers of adducted maleic anhydride on one molecule of the fractions were calcu-

TABLE III Some analyses of PS fractions prepared from PI fractions after the Diels–Alder reaction

Sample	Reaction conditions	PS yield[a] (wt %)	Element (wt %)				H/C	O/C ($\times 10^{-1}$)	M_n[b]	Adducted MA[c]
			C	H	O	Diff.				
PMP-PI	175 °C,1 h	73	80.4	4.0	13.8	1.8	0.60	1.29	2520	7.2
NMP-PI	150 °C,1 h	74	74.3	4.3	20.5	0.9	0.69	2.07	1740	7.4

[a] Based upon the starting PI fraction.
[b] Average molecular weight by VPO.
[c] Molar number of the adducted maleic anhydride (MA) in the fraction calculated from elemental analyses and molecular weight.

TABLE IV Structural parameters of PS fractions after correction of adducted maleic anhydride

Sample	Elemental composition composition	M_n[b]	Hydrogen distribution (%)[c]				Brown–Ladner analyses			
			H_{ar}	H_α	H_β	H_r	f_a[d]	σ_{al}[e]	R_{tus}/R_{tus}[f]	H_a/C_a[g]
PMP-PI	$C_{143}H_{89}$	1814	63.7	24.6	8.5	3.2	0.89	0.16	0.14	0.51
NMP-PI	$C_{80}H_{60}$	1015	60.7	25.6	10.5	3.3	0.85	0.17	0.22	0.59

[a] Estimated by subtraction of the adducted maleic anhydride.
[b] Average molecular weight.
[c] H-NMR, chemical shift (ppm) Har: 6 ~ 10, Hd: 1.7–4.3, H_e: 1.0 ~ 1.7, H_α: 0.3 ~ 1.0
[d] Carbon aromaticity.
[e] Degree of aliphatic sub-units per unit structure.
[f] Ratio of the naphthenic ring in the aromatic structure.
[g] Ratio of the aromatic hydrogen and carbon in the unit structure.

lated to be above 7 in both fractions, based on the analyses.

The elemental composition, average molecular weight, hydrogen distributions and some Brown–Ladner structural parameters of the parent PI fractions are summarized in Table IV. Such parameters were corrected by substracting the contribution of the adducted maleic anhydride to the solubilized PI, based on its molar number estimated as above. The average molecule in PMP-PI has $C_{145}H_{89}$ (molecular weight 1814) and Brown–Ladner parameters such as carbon aromaticity, $f_a = 0.89$, degree of aliphatic substitution, $\sigma_{al} = 0.16$, number of naphthenic ring/total number of ring, $R_{nus}/R_{tus} = 0.14$, aromatic H/C atomic ratio, $H_a/C_a = 0.51$. The average molecule in NMP-PI has $C_{80}H_{60}$ (molecular weight 1015), $f_a = 0.85$, $\sigma_{al} = 0.17$, $R_{nus}/R_{tus} = 0.22$, and $H_a/C_a = 0.59$. Such parameters of the solubilized fractions suggest that PMP-PI carries larger molecules of highly peri-condensed rings, less aliphatic and naphthenic groups, than NMP-PI.

4. Discussion

The present study revealed that the components in the pyridine-insoluble fractions of both mesophase pitches derived from FCC–DO and naphthalene are reactive with maleic anhydride in the Diels–Alder reaction. The components in the mesophase pitch which were believed to consist of polycondensed aromatic rings [1, 2, 8–15] carry the reaction sites for the Diels–Alder reaction. The reaction was found to introduce the carbonyl and ether groups by eliminating the isolated aromatic C–H bonds by adducting the maleic anhydride. On average, seven molecules of the maleic anhydride are introduced into a mesophase molecule. The Diels–Alder reaction is suggested to proceed through dissolving the PI particle in the melted maleic anhydride.

The introduced maleic anhydride should increase the solubility of mesophase molecules in polar solvents because of the polarity introduced through the adducted maleic anhydride and bent structure of the adduct. The small and soluble molecules trapped in the large mesophase molecules may be released because of the dissolving ability of the maleic anhydride during the reaction. Hence, high solubility up to 90 wt % in pyridine was achieved by this kind of Diels–Alder reaction at 175–200 °C.

Such a modification of the structures of mesophase pitch molecules may sterically hinder the layered stacking, although the PI fractions before and after the Diels–Alder reaction showed similar optical anisotropy, stacking height, $L_c(002)$, and $d(002)$ spacing.

It is of greater worth to discuss the optical anisotropy and molecular stacking associations which were certainly restored even after the Diels–Alder reaction. The introduced maleic anhydride in the mesophase molecules may not disturb the alignment and *c*-axial stacking of the molecules and the regularity as a liquid crystal. Nevertheless, such molecular assembles carrying a non-planar structure in the liquid-crystal mesophase pitch may influence their molecular arrangements in the spun fibre, some changes in properties of their resultant carbon fibres being expected [22, 23]. Unfortunately, no spinning is allowed at present because of retro-Diels–Alder reaction at the spinning temperature.

The increased solubility of PI fraction allowed detailed analysis of their chemical structures. Based on Brown–Ladner parameters, infrared spectroscopy, and molecular weight, some representative molecules in PI fractions in FCC-DO and naphthalene-derived mesophase pitches are illustrated in Figs 8 and 9,

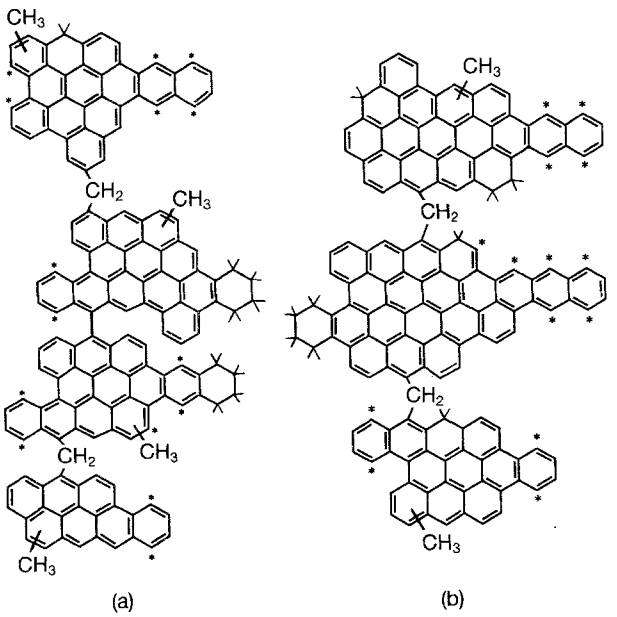

Figure 8 Model structures of the PMP-PI fraction. (*) Reactive sites for the Diels–Alder reaction.

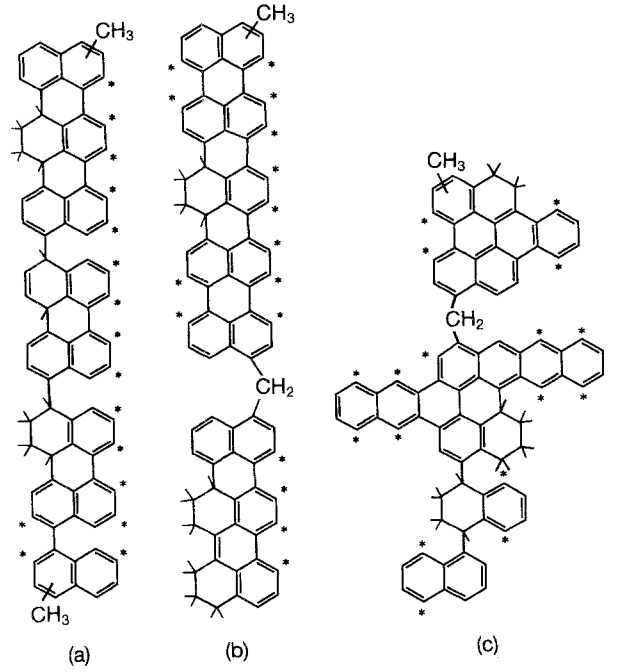

Figure 9 Model structures of the NMP-PI fraction. (*) Reactive sites for the Diels–Alder reaction.

respectively. The mesophase molecules in the present two pitches are very different in terms of structure, probably reflecting their starting substances and the preparation conditions.

PMP-PI carries larger aromatic rings of very peri-condensed structures with fewer numbers of aliphatic and naphthenic groups than NMP-PI. It should be noted that PMP-PI has a greater number of methylene and aryl–aryl linkages between the aromatic units for its higher molecular weight. Such structures are basically similar to those observed with the soluble components of the same mesophase pitches as reported in previous papers [6, 9–12, 24–27], although the molecular weight and size of aromatic nucleus units are certainly larger.

The model structures illustrated in Figs 8 and 9 carry pairs of isolated aromatic C–H designated by the asterisk. Such sites may react with maleic anhydride in the Diels–Alder reaction as suggested by the organic model compounds such as naphthalene, anthracene, and perylene [28–31]. Peri-type ring arrangement in PMP-PI may have more 9,10 and 1,4 positions of anthracene units, the former of which is very reactive in the Diels–Alder reaction. The reaction may start at positions 9 and 10 at lower temperatures, while positions 1 and 4 are much less reactive, reacting at higher temperatures.

NMP-PI consists basically of perylene units, of which 1,4 and 3,6 positions are reactive, as the reaction of perylene suggests. The uniformity of the reaction sites in the fraction may lead to a narrower temperature range for the initiation and completion of the reaction.

References

1. I. MOCHIDA and Y. KORAI, *J. Fuel Soc. Jpn.* **64** (1985) 796.
2. I. MOCHIDA, H. TOSHIMA, Y. KORAI and T. MATSUMOTO, *J. Mater. Sci.* **23** (1988) 670.
3. I. MOCHIDA, H. TOSHIMA, Y. KORAI and T. NAITO, *ibid.* **23** (1988) 678.
4. I. MOCHIDA, H. TOSHIMA, Y. KORAI and T. MATSUMOTO, *ibid.* **24** (1989) 57.
5. I. MOCHIDA, H. TOSHIMA, Y. KORAI and T. HINO, *ibid.* **24** (1989) 389.
6. I. MOCHIDA, H. TOSHIMA, Y. KORAI and T. MATSUMOTO, *ibid.* **25** (1990) 76.
7. I. MOCHIDA, S. M. ZENG, Y. KORAI, T. HINO and H. TOSHIMA. *Carbon* **29** (1991) 23.
8. I. MOCHIDA and Y. KORAI, *Kobushi* **35** (1986) 456.
9. I. MOCHIDA, K. SHIMIZU, Y. KORAI, H. OTSUKA and S. FUJIYAMA, *Carbon* **28** (1990) 311.
10. I. MOCHIDA, K. SHIMIZU, Y. KORAI, H. OTSUKA, S. FUJIYAMA and Y. SAKAI *ibid.* **28** (1986) 311.
11. Y. D. PARK, Y. KORAI and I. MOCHIDA, *J. Mater. Sci* **21** (1986) 424.
12. I. MOCHIDA, Y. KORAI, A. AZUMA, M. KAKUTA and E. KITAJIMA, *ibid.* **26** (1991) 4836.
13. L. REGGLE, R. RAYMOND, R. A. FREIDMAN and I. WENDER, *Fuel* **37** (1958) 126.
14. I. MOCHIDA, K. MAEDA and K. TAKESHITA, *Carbon* **15** (1977) 17.
15. *Idem, ibid.* **16** (1978) 459.
16. G. ZHERAKOVA and R. KOCHKANAN, *Fuel* **69** (1990) 898.
17. M. NISHIOKA and J. W. LARSEN, *Energy Fuel* **4** (1990) 100.
18. T. IZUMI, Jpn Pat. 58-180585 (1983).
19. 117 Committee of Japan Society for the Promotion of Science, *Tanso* **36** (1963) 25.
20. J. K. BROWN and W. R. LADNER, *Fuel* **39** (1960) 79.
21. T. KATO, H. ITO, K. OUCHI and J. SOHMA, *J. Fuel Soc. Jpn* **55** (1976) 244.
22. I. MOCHIDA, K. SHIMIZU, Y. KORAI, Y. SAKAI, S. FUJIYAMA, H. TOSHIMA and T. HINO, *Carbon* **26** (1992) 55.
23. Y. KORAI and I. MOCHIDA, in "Proceedings of 20th Biennial Conference on Carbon", Santa-Barbara, CA (American Carbon Society, 1991) p. 148; *Carbon*, in press.
24. I. MOCHIDA, H. TOSHIMA, Y. KORAI and T. VARGA, *J. Mater. Sci.* **25** (1990) 3438.
25. Y. KORAI and I. MOCHIDA, *Carbon* **23** (1985) 97.
26. I. MOCHIDA, K. SHIMIZU, Y. KORAI, Y. SAKAI, S. FUJIYAMA, H. TOSHIMA and T. HINO, *ibid.* **30** (1992) 55.
27. Y. KORAI, M. NAKAMURA, I. MOCHIDA, Y. SAKAI and S. FUJIYAMA, *ibid* **29** (1991) 561.

28. E. CLAR and M. ZANDER, *J. Chem. Soc.* **65** (1957) 4616.
29. Y. ALTMAN and D. GINSBURG, **67** (1959) 4660.
30. A. A. DANISH, M. SILVERMAN and Y. A. TAJIMA, *J. Am. Chem. Soc.* **76** (1954) 6144.
31. J. A. NORTON, *Chem. Rev.* **31** (1942) 319.

Received 23 September 1992
and accepted 27 September 1993